NASA SP-315

APOLLO 16

Preliminary Science Report

PREPARED BY

NASA MANNED SPACECRAFT CENTER

Scientific and Technical Information Office 1972

NATIONAL AERONAUTICS AND SPACE ADMINISTRATION

Washington, D.C.

19. X-Ray Fluorescence Experiment

I. Adler,[a†] J. Trombka,[a] J. Gerard,[ab] P. Lowman,[a] R. Schmadebeck,[a]
H. Blodget,[a] E. Eller,[a] L. Yin,[a] R. Lamothe,[a] G. Osswald,[a] P. Gorenstein,[c]
P. Bjorkholm,[c] H. Gursky,[c] B. Harris,[c] L. Golub,[c] and F. R. Harnden, Jr.[c]

The X-ray fluorescence spectrometer, carried in the scientific instrument module bay of the command and service module, was used for orbital mapping of the lunar surface composition and X-ray galactic observations during transearth coast. The lunar surface measurements involved observations of the intensity and characteristic energy distribution of the secondary or fluorescent X-rays produced by the interaction of solar X-rays with the lunar surface. The astronomical observations consisted of relatively long periods of X-ray measurement of preselected galactic sources such as Cygnus (Cyg X-1) and Scorpius (Sco X-1).

COMPOSITIONAL MAPPING OF THE LUNAR SURFACE

The lunar surface was mapped with respect to magnesium (Mg), aluminum (Al), and silicon (Si) as Al/Si and Mg/Si ratios along the projected ground tracks by the orbiting Apollo 16 spacecraft. The results confirm the Apollo 15 observations and provide new data for several features not previously covered. The data are consistent with the theory that the Moon has a widespread differentiated crust (the highlands). The Al/Si and Mg/Si chemical ratios of the highlands correspond to those of anorthositic gabbro and gabbroic anorthosite. The X-ray results suggest that this premare crust or material similar to it occurs at the Descartes landing site.

Unlike the high inclination orbit of the Apollo 15 spacecraft, the Apollo 16 flightpath was nearly equatorial (9° inclination) so that the areas covered were somewhat smaller than those of the Apollo 15 flight. Although the original flight plan called for a plane change, the circumstances of the mission did not permit this. Consequently, some of the ground coverage was lost.

Theoretical Basis

The theoretical basis for the X-ray fluorescence experiment and a description of the instrument have been given in some detail previously (refs. 19-1 to 19-3). Briefly, the experiment involves orbital measurements of the characteristic secondary X-rays produced by the interaction of the solar X-rays with the lunar surface. Because of the spectral nature of the solar flux, the measurements are limited to the K-shell spectra of the elements Mg, Al, and Si. The heavier elements are not appreciably excited, and the elements lighter than Mg are inefficiently detected. Furthermore, the measurements are limited to that part of the lunar surface that is illuminated by the Sun.

Description of the Instrument

The Apollo 16 instrument is essentially identical to that flown on the Apollo 15 mission and consists of three main subsystems (fig. 19-1).

(1) Three large-area proportional counters that have state-of-the-art energy resolution and 0.0025-cm-thick beryllium windows

(2) A set of large-area filters for energy discrimination among the characteristic X-rays of Al, Si, and Mg

(3) A data handling system for count accumulation, for sorting into eight pulse-height channels, and for relaying the data to the spacecraft telemetry

The X-ray detector assembly consists of three proportional-counter detectors, two X-ray filters, mechanical collimators, an inflight calibration device, temperature monitors, and associated electronics. The detector assembly senses X-rays that are emitted from

---

[a]NASA Goddard Space Flight Center.
[b]National Academy of Sciences.
[c]American Science and Engineering.
†Principal Investigator.

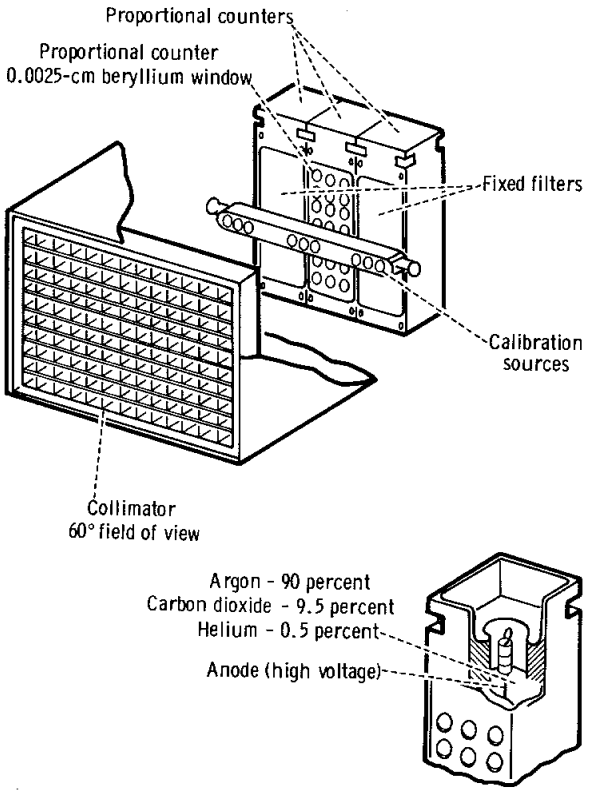

FIGURE 19-1.–Functional configuration of the X-ray spectrometer.

the lunar surface and converts the X-rays to voltage pulses which are processed in the X-ray processor assembly. Provisions for inflight calibration are made by means of programed calibration sources, which, upon internal command, assume a position in front of the three detectors for calibration of gain, resolution, and efficiency. Thermistors, which are located at strategic points, sense the temperature of the detector assembly for telemetry monitoring and temperature control of the detectors by means of heaters located near the proportional-counter windows.

The behavior of the X-ray output of the Sun was simultaneously monitored with the lunar surface measurements by means of the solar monitor, a small proportional detector mounted on the opposite side of the spacecraft from the surface detectors. On the Apollo 16 spacecraft, a thin beryllium foil filter was added in front of the detector window to enable the spectrometer to view high-Sun X-ray fluxes without experiencing the detector gainshifts that were observed during the Apollo 15 flight.

Operation of the Experiment

The X-ray experiment began to function on April 20, 1972, at approximately 02:00 Greenwich mean time (G.m.t.) and was operated for approximately 12 hr in an elliptical orbit (approximately 10 by 60 n. mi.). At approximately 04:00 G.m.t. on April 21, the experiment was again activated; the spacecraft was in a circular lunar orbit of approximately 60 n. mi. As in the Apollo 15 flight, the estimated field of view for each data point used in this report is approximately 60 by 80 n. mi. The data were reduced during the mission. Thus, conclusions about the Descartes landing site could be made and reported to the crewmen while they were on the surface.

The overlap of orbital coverage between the Apollo 15 and 16 ground tracks (mainly from 50° to 100° E) makes it possible to compare the reproducibility of the measurements for both missions. The total coverage for the two missions is greater than 20 percent of the surface of the Moon. The Apollo 16 spectrometer provided data for a number of features not previously covered; for example, Mare Cognitum, Mare Nubium, Ptolemaeus, Descartes, and Mendeleev as well as several other areas (fig. 19-2). It is encouraging that, for these areas, the Al/Si and Mg/Si chemical ratios for both flights agreed to better than 10 percent (table 19-I). This agreement makes it possible to draw comparisons between the two flights. It also demonstrates that the X-ray spectral distribution of the Sun, which produces lunar fluorescent X-rays, was about the same on both missions. In fact, this conclusion has been confirmed by examination of the SOLRAD data[1] available for those periods. Another point of considerable interest is that the spectrometer obtained a large number of data points over the Descartes landing site (fig. 19-2 and tables 19-II and 19-III). Hopefully, the results will show how representative the data are of the Descartes area.

Results and Observations

The following preliminary results and observations are based on the reduction of the data tapes supplied

[1]The SOLRAD data are obtained by satellite monitoring solar radiation and are reported by the National Oceanic and Atmospheric Administration, Rockville, Maryland, in Solar-Geophysical Data (Prompt Reports).

TABLE 19-I.–Overlap Between the Apollo 15 and 16 Ground Tracks

Feature (a)	Apollo 16 concentration ratio		Apollo 15 concentration ratio	
	Al/Si ± 1σ	Mg/Si ± 1σ	Al/Si ± 1σ	Mg/Si ± 1σ
Mare Fecunditatis	0.41 ± 0.05	0.26 ± 0.05	0.36 ± 0.06	0.25 ± 0.03
Mare Smythii	.45 ± .08	.25 ± .05	.45 ± .06	.27 ± .06
Langrenus area	.48 ± .07	.27 ± .06	.48 ± .11	.24 ± .06
Highlands west of Smythii	.57 ± .07	.21 ± .03	.55 ± .06	.22 ± .03
Western border of Smythii	.58 ± .08	.22 ± .04	.52 ± .06	.22 ± .06
Eastern border of Smythii	.61 ± .09	.20 ± .06	.60 ± .10	.21 ± .03

[a]The overlap between corresponding areas of the Apollo 16 and 15 ground tracks is not exact, so that differences for the same area may be real (fig. 19-2).

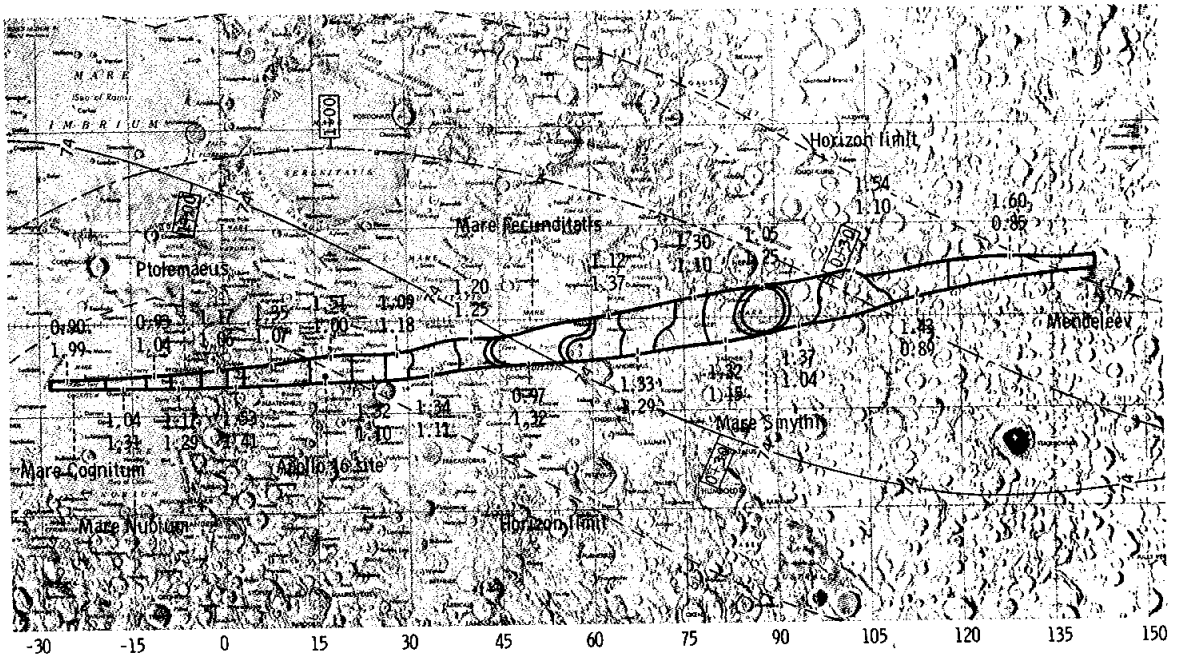

FIGURE 19-2.–Al/Si and Mg/Si intensity ratios for specific areas along the Apollo 16 ground tracks. The first values are Al/Si and the second values are Mg/Si. The double lines represent the transition zones between the mare basins and the highlands. The intensity ratios in these zones reflect an overlap between the lower mare values and the higher highland values.

during the Apollo 16 mission. For the most part, the data points represent 64-sec accumulations, so that the surface spatial resolution is not optimal. The reduced data have been treated in several ways. The Al/Si and Mg/Si intensity ratios have been plotted along the ground tracks and related to gross features as well as other phenomena such as optical albedo. (The refined data will be treated at shorter intervals and published subsequently.)

Figure 19-2 shows the variation of Al/Si and Mg/Si intensity ratios plotted along the projected Apollo 16 ground tracks. These ground tracks have been divided into areas based in part on obvious geologic features and in part on intensity contours. Because of the relatively low inclination of the orbit and the repetitive ground tracks, there is a high

TABLE 19-II.–Concentration Ratios of Al/Si and Mg/Si for Various Features

Feature	N (a)	Concentration ratio	
		Al/Si ± 1σ	Mg/Si ± 1σ
Mare Cognitum	8	0.38 ± 0.11	0.40 ± 0.29
Upper part of Sea of Clouds (9° to 13° W)	8	.39 ± .12	.20 ± .05
Mare Fecunditatis (42° to 57° E)	80	.41 ± .05	.26 ± .05
South of Fra Mauro (13° to 19° W)	9	.45 ± .07	.26 ± .04
Mare Smythii (82° to 92.5° E)	24	.45 ± .08	.25 ± .05
Southern edge of Mare Tranquillitatis, Torricelli area (26° to 30° E)	21	.47 ± .09	.23 ± .05
Eastern edge of Fecunditatis, Langrenus area (57° to 64° E)	44	.48 ± .07	.27 ± .06
Ptolemaeus (4° W to 0.5° E)	17	.51 ± .07	.21 ± .04
Highlands west of Ptolemaeus to Mare Nubium (4° to 9° W)	16	.51 ± .11	.25 ± .12
Highlands west of Mare Fecunditatis (37.5° to 42° E)	29	.52 ± .07	.24 ± .05
Highlands west of Smythii (72° to 77° E)	35	.57 ± .07	.21 ± .03
Western border of Smythii (77° to 82° E)	33	.58 ± .08	.22 ± .04
Highlands east of Descartes (20.5° to 26° E)	23	.58 ± .07	.21 ± .04
South of Mare Spumans (64° to 72° E)	45	.58 ± .07	.25 ± .04
Isidorus and Capella (30° to 37.5° E)	38	.59 ± .11	.21 ± .05
Highlands west of Descartes (3° to 14° E)	44	.59 ± .11	.21 ± .05
Eastern border of Mare Smythii (92.5° to 97.5° E)	17	.61 ± .09	.20 ± .06
Far-side highlands (106° to 118° E)	29	.63 ± .08	.16 ± .05
Descartes area, highlands, Apollo 16 landing site (14° to 20.5° E)	30	.67 ± .11	.19 ± .05
East of Ptolemaeus (0.5° to 3° E)	12	.68 ± .14	.28 ± .09
Highlands (97.5° to 106° E)	31	.68 ± .11	.21 ± .05
Far-side highlands west of Mendeleev (118° to 141° E)	30	.71 ± .11	.16 ± .04

[a]N is the number of individual data points used to determine the average Al/Si and Mg/Si values ±1 standard deviation and was obtained from the various passes over each feature.

density of plotted data points. Thus, each value shown represents the average of a substantial number of points.

Detailed results expressed as concentration ratios are given in tables 19-II and 19-III. A brief summary of the main observations follows.

(1) The early reports of very high Al/Si ratios in the Descartes area, given while the mission was in progress, have been confirmed by the analysis of some of the returned lunar samples. The value of 25 to 29 percent aluminum oxide, reported in reference 19-5, agrees very well with the preliminary estimate of 26 to 27 percent. From figure 19-2, it appears reasonable that some of the material sampled at Descartes may be similar to the eastern limb and far-side highlands. This conclusion is further justified by the fact that the Mg/Si concentration ratio for some of the returned material is approximately 0.18, close to the anticipated value of 0.19 ± 0.05. The Mg/Si concentration ratios for the eastern limb and far-side highlands are approximately 0.16 to 0.21 (tables 19-II and 19-III).

(2) The Apollo 15 observations of high Al and low Mg values in the highlands and the reverse in the mare areas are confirmed by the Apollo 16 data. However, there are exceptions. For example, the area east of Ptolemaeus has both high Al/Si and Mg/Si ratios.

(3) In both missions, the Al and Mg values show an inverse relationship, although this is not true

TABLE 19-III.–Concentration Ratios of Al/Si and Mg/Si for Selected Lunar Samples

Selected lunar samples	Concentration ratio		Reference
	Al/Si	Mg/Si	
Apollo 12, Oceanus Procellarum type AB rocks, average	0.22	0.22	19-4
Apollo 15, Hadley-Apennine rocks, average	.22	.27	19-5
Apollo 12, Oceanus Procellarum type B rocks, average	.22	.37	19-4
Apollo 11, Mare Tranquillitatis high potassium rocks, average	.23	.24	19-6
Apollo 12, Oceanus Procellarum type A rocks, average	.24	.31	19-4
Apollo 12, rock 12013	.24 to .30	.20	19-4
Apollo 11, Mare Tranquillitatis low potassium rocks, average	.29	.23	19-6
Apollo 12, dark portion of rock 12013	.33	.22	19-7, 19-8
Apollo 12, Oceanus Procellarum soil, average	.33	.29	19-4
Surveyor VI, Sinus Medii regolith	.34	.20	19-9, 19-10
Apollo 15, Hadley-Apennine soil	.34	.30	19-5
Surveyor V, Mare Tranquillitatis regolith	.35	–	19-10, 19-11
Luna 16, Mare Fecunditatis rocks	.35	.21	19-12
Apollo 11, Mare Tranquillitatis bulk soil, average	.37	.24	19-6
Apollo 14, Fra Mauro rocks, average	.38	.26	19-13
Apollo 11 and 12, potassium, rare-Earth elements, and phosphorus (KREEP), average	.39	.21	19-7, 19-8
Apollo 14, Fra Mauro soil	.41	.26	19-13
Apollo 12, norite material, average	.42	.20	19-14, 19-15
Luna 16, Mare Fecunditatis bulk soil	.42	.27	19-12
Surveyor VII, rim of Tycho, regolith	.55	.20	19-10, 19-16
Luna 20, Apollonius Highlands	.58	.26	19-12
Apollo 11 and 12, anorthositic gabbro	.64	.21	19-14, 19-15
Apollo 15, rock 15418, gabbroic anorthosite	.67	.15	19-5
Apollo 11 and 12, gabbroic anorthosite	.82	.074	19-14, 19-15
Apollo 11 and 12, anorthosite	.89	.038	19-14, 19-15
Apollo 15, rock 15415, anorthosite, Genesis Rock	.91	.003	19-5

everywhere.

Figures 19-3 and 19-4 show detailed plots of Al/Si and Mg/Si values (intensities and concentration ratios) as compared to longitude for the projected Apollo 16 ground track. Various mare and highland features are identified. Analyzed material is shown for reference on the left-hand concentration scale. Marked differences exist between the highland and mare areas. For example, the extreme variation in Al/Si concentration is almost a factor of 2 between the low values in Mare Cognitum and the high values in the highlands west of Mendeleev. The Mg/Si ratios vary inversely, with the Al/Si ratios being highest in the mare and lowest in the highlands.

One of the results to emerge from the Apollo 15 mission was the excellent correspondence between the Al/Si values and the optical albedo values. This observation was particularly significant in view of the long-standing discussion as to whether these albedo differences were solely representative of topographic differences or were also a reflection of compositional differences among surface materials. Early investigators, such as Whitaker (ref. 19-17), recognized convincing evidence for compositional changes where sharp albedo changes occur. However, it remained for the later Surveyor, Luna, Lunokhod, and Apollo

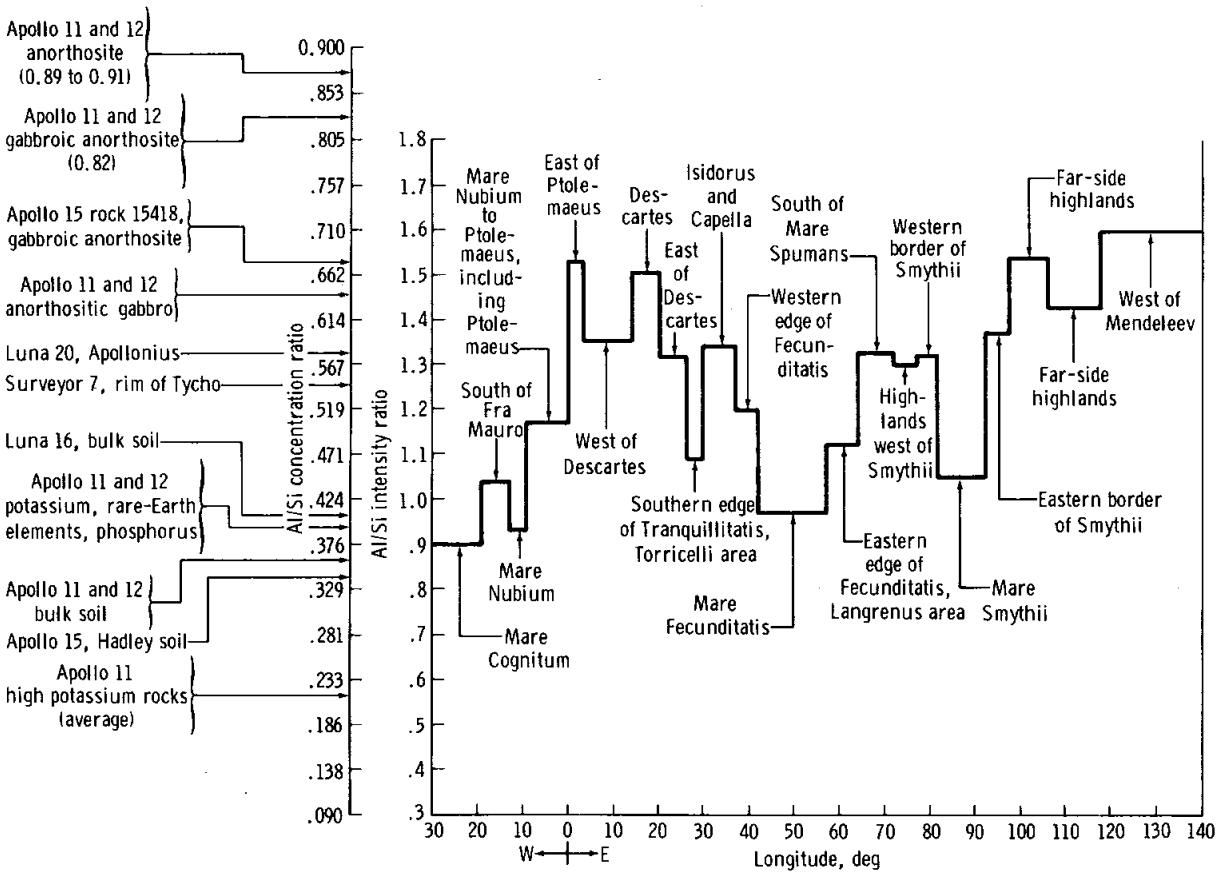

FIGURE 19-3.–Al/Si intensity and concentration ratios as compared to longitude.

missions to provide quantitative compositional data. Chemical differences related to the albedo were first confirmed by the alpha scattering experiments of Surveyor V, VI, and VII. The Surveyor V soft lander tested widely separated mare sites and reported chemically similar surfaces for each. Surveyor VII, on the other hand, returned samples from a highland site; significant chemical differences between the highlands and the two mare locations were reported (ref. 19-18). The Surveyor results and analyses of returned lunar samples confirmed that albedo is indeed affected by compositional as well as topographic differences. The X-ray fluorescence experiment on the Apollo 15 and 16 missions has now provided the means to correlate regional albedo with surface composition (for selected elements).

Data locations for selected Apollo 15 and 16 orbits covered by the X-ray fluorescence experiment were plotted on the map of the normal albedo of the Moon by Pohn, Wildey, and Sutton (ref. 19-19). Average albedo was then computed for each 3° area for which the X-ray data were available and plotted against the Al/Si intensity ratios. The positive correlation between the albedo and Al/Si values is strong, although the rate of change is not always similar. In the Apollo 15 plots, the main anomalies were observed where an occasional small Copernican crater occurred, which produced an abnormally high albedo value. The brightness of these craters is generally considered to be due to the highly reflective, finely divided ejecta rather than compositional changes. A similar anomaly is noted in the Apollo 16 data at approximately 27° E in a Tranquillitatis embayment north of Theophilus. Four Apollo 16 revolutions were plotted (fig. 19-5), and revolutions 58 and 60 show the expected decrease in Al/Si values with decreasing albedo. Revolutions 55 and 59, on the other hand, show an occasional increase in Al/Si values although the albedo decreases. This may record the existence of old "weathered" rays consisting of

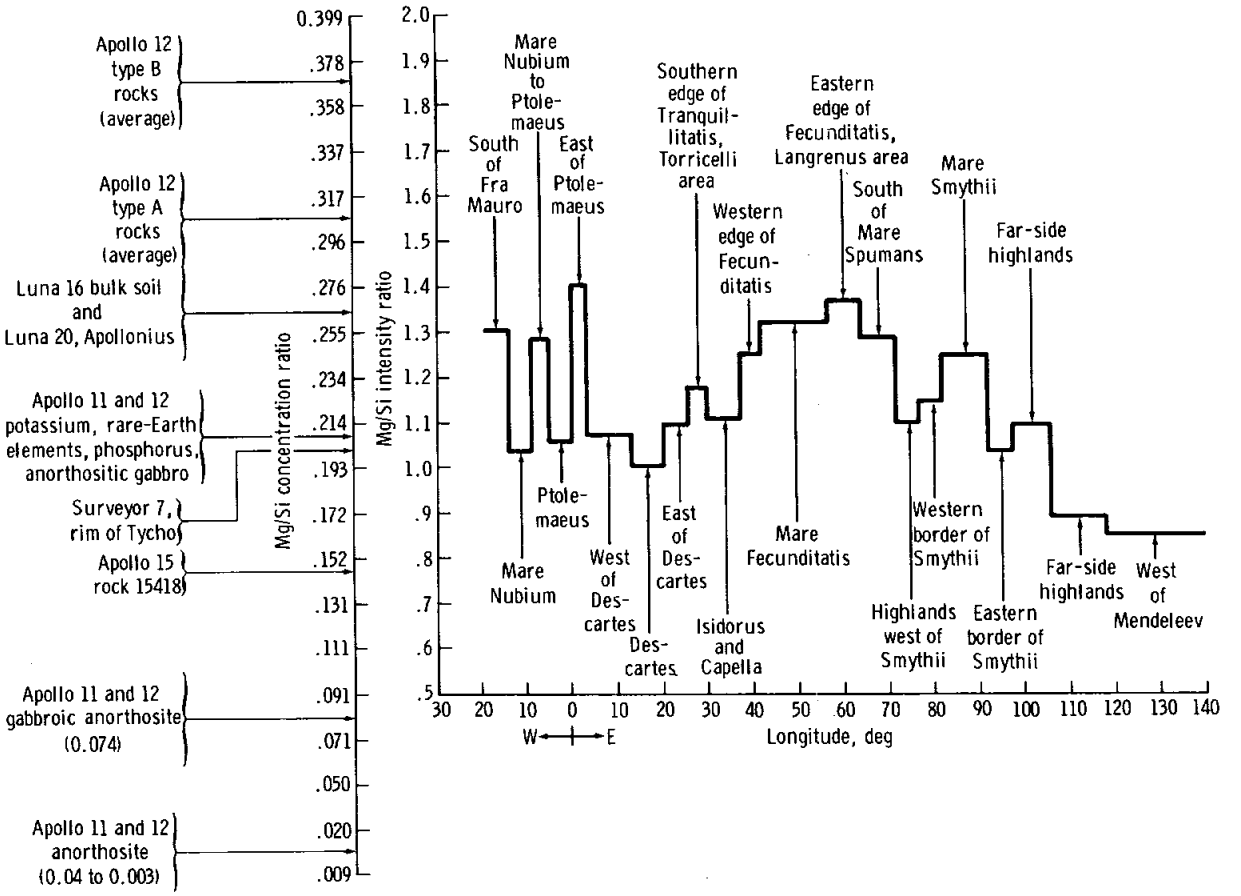

FIGURE 19-4.–Mg/Si intensity and concentration ratios as compared to longitude.

aluminum-rich highland-derived ray material that has now lost its high reflectivity.

Geologic Interpretation

The results of the Apollo 16 X-ray fluorescence experiment generally support the main conclusions reached after the Apollo 15 mission (ref. 19-2). However, further conclusions are now possible.

First, and most important, the good correlation between the aluminum oxide content inferred from the X-ray data and the returned samples implies that the X-ray measurements are a reliable guide, at least to this aspect of the surface composition of the Moon. Second, the strong correlation between albedo and Al/Si ratios suggests that, if allowance is made for features the brightness of which is primarily caused by physiographic youth (such as Copernican craters), the albedo is a reasonable guide to highland composition, specifically to its plagioclase content. Together, these conclusions imply that the plagioclase-rich highland crust, the existence of which was first inferred from the Apollo 11 samples, is global in extent, although albedo measurements are not yet available from the far side of the Moon.

The data from the highland area covered by the Apollo 16 spectrometer have maximum Al/Si ratios that lie between those of anorthositic gabbro and gabbroic anorthosite returned from previous Apollo missions (fig. 19-3). Despite the frequent occurrence of anorthositic fragments in regolith samples, nowhere are the Al/Si ratios as high as those of anorthosite. This high ratio implies that anorthosite is a subordinate though widespread constituent of the highland crust, the bulk of which is anorthositic gabbro (using the term in a chemical sense). Local concentrations of anorthosite could form by crystal flotation from a gabbroic magma; how the magma itself formed is not clear.

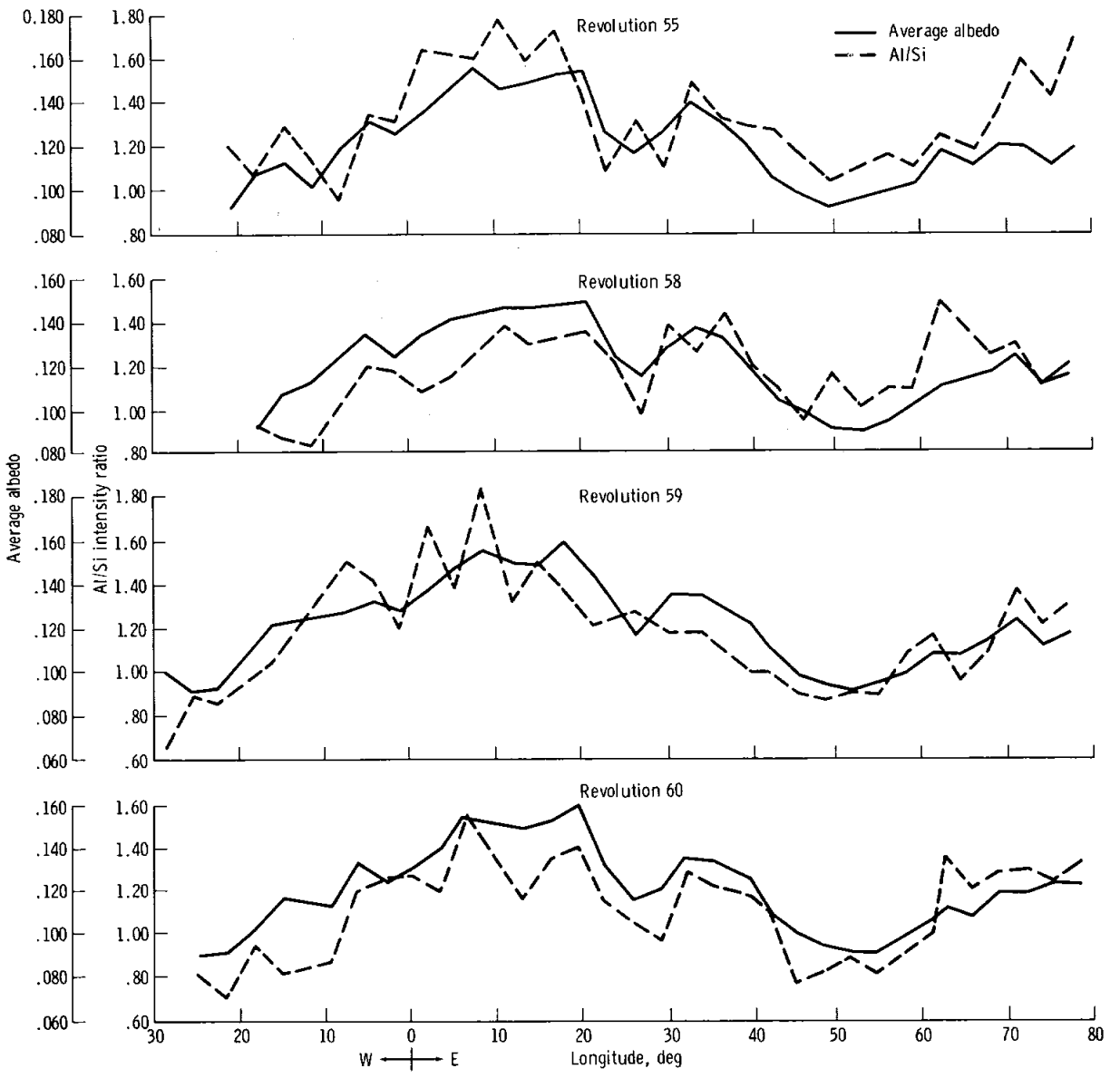

FIGURE 19-5.–Al/Si intensity ratios as compared to optical albedo for revolutions 55, 58, 59, and 60.

The good correlation between optical albedo and aluminum (or plagioclase) content suggests an explanation for the unexpected abundance of breccias in the Apollo 16 samples of the Descartes Formation. This formation had been interpreted as volcanic flows and pyroclastics (refs. 19-20 and 19-21); Head and Goetz had considered the Descartes Formation to be partially of Copernican age because of its high albedo content and other characteristics. Such a young unit would not be expected to be extensively brecciated by small impacts, as are older lunar rocks. However, the X-ray fluorescence/albedo correlation suggests that the high albedo content may be the expression of a high plagioclase content, as might be found in a local anorthositic occurrence, rather than a Copernican age. The Descartes Formation might then be much older than had been expected, and the abundance of breccias would therefore be understandable.

Summary

The Apollo 16 X-ray fluorescence experiment has been successful, confirming earlier results from the Apollo 15 mission and providing compositional data over new areas of the Moon. The data are still being analyzed and integrated with information from other remote sensing experiments and returned sample analyses. However, the data have so far provided further confirmation of the existence of an extensive lunar crust consisting largely of what may be anorthositic gabbro. This crust, which was probably global in extent before formation of the mare basins, is of broad scientific interest in that it represents an early period of planetary differentiation of which virtually no direct evidence remains on the Earth. Additional study of both X-ray data and their implications is therefore highly desirable.

GALACTIC X-RAY OBSERVATIONS

Objectives and Theory

During transearth coast, the X-ray fluorescence spectrometer was used to observe the temporal behavior of two pulsating X-ray sources within our galaxy. The Apollo 16 studies of time variations in the output of galactic X-ray sources were a continuation of an observational program that began with the Apollo 15 mission. (There is an introductory discussion on the scientific objectives and theoretical basis of the observations in ref. 19-2.)

As a result of advances in the understanding of the nature of pulsating X-ray sources, it was decided that the Apollo 16 experiment should concentrate on the two most intense sources, Sco X-1 and Cyg X-1. Sco X-1 has been identified with a visible and radio star; since the Apollo 15 mission, a good case has been made for identifying Cyg X-1 with a ninth-magnitude BO supergiant, which is also a spectroscopic binary star (refs. 19-22 and 19-23). Therefore, it was planned to make coordinated observations from the Apollo 16 spacecraft and ground-based observatories on both Sco X-1 and Cyg X-1 in X-rays, visible light, and radio wavelengths, simultaneously or nearly simultaneously.

The primary objective of the Apollo 16 transearth coast studies was to measure the temporal variation of the X-ray luminosity of Sco X-1 and Cyg X-1 in the time regime from 8 sec (the minimum time resolution of the instrument) to 2 hr (the maximum time of a celestial pointing position), and to correlate it with radio and optical activity. A secondary objective was to study the cislunar space environment as a site for pointed X-ray astronomy observations. Specifically, the objective was to determine how the soft particle background in the X-ray detectors from trapped electrons or protons in cislunar space compared to the near-Earth and lunar environments. During data reduction, it became necessary to study the pointing stability of the command and service module during long periods. Data analysis from the standpoint of these secondary objectives may be useful in planning future observations from other spacecraft.

Operation of the Experiment

Operation of the experiment consists of steadily pointing the X-ray fluorescence spectrometer at a fixed celestial location for the entire interval of 1 to 2 hr. The instrument was intentionally pointed approximately 7° away from both Sco X-1 and Cyg X-1 to avoid a significant contribution from other known X-ray sources. It is important to minimize spacecraft motion, because it results in spurious temporal variations in count rate. The instrument has an angular-dependent intensity response as a result of the effect of the collimator, its field of view being 30° full width, half maximum (FWHM) in two directions. (The FWHM is the total angular width at which the collimator drops to one-half of its peak response.) The spacecraft was commanded to maintain the finest pointing control possible to avoid spurious variations in count rate. A 10.5-hr period of pointed X-ray data was obtained. The total observation time obtained was about equal to the amount planned prior to the mission.

Arrangements were made with a network of ground-based observatories to cover Sco X-1 and Cyg X-1 at various times during the Apollo 16 mission. At any particular time, only a limited number of observatories are in a favorable position. In principle, a broad geographic distribution would cover all observations. The cooperating optical observatories included the Crimean Astrophysical Observatory (U.S.S.R.), the Leyden Observatory (South Africa), the Wise Observatory (Israel), the McDonald Observatory (U.S.A.), and the Yerkes Observatory (U.S.A.). The radio facilities were the Westerbork Observatory

(the Netherlands), the Algonquin Observatory (Canada), and the National Radio Astronomy Observatory (U.S.A.).

The fact that the beginning of transearth coast occurred approximately 1 day earlier than was planned did create difficulties for the coordinated observation program with ground-based observatories. As changes in the flight plan occurred, participating ground observatories were asked to adjust their schedules to maintain near simultaneity with Apollo 16 observations. However, in many cases, the observatories were not able to do so; thus, not as much near-simultaneous optical and radio coverage was obtained as was anticipated. In addition, bad weather conditions at the Crimean Astrophysical Observatory prevented their observations.

The spectrometer performed very well throughout transearth coast. Deep space pointing attitudes for periods of 2 hr did result in low temperatures in the vicinity of the instrument. However, judging from the calibration sources, the experiment heaters did maintain the instrument in a proper operating condition.

Recent Developments in Pulsating X-Ray Sources

During the time between the Apollo 15 and 16 missions, much was learned from Explorer 42 (UHURU) observations about the nature of pulsating X-ray sources. It is clear that there are several classes. One class is characterized by a highly regular period of several seconds plus additional periods of several days (ref. 19-24). Centaurus (Cen X-3) is an example of this class. The parameters of the class definitely require a binary system, possibly involving a low mass star. In terms of observations, if not in theory, such regular pulsating systems are comparatively well understood. However, their characteristic periods are not in a time regime suitable for study by the X-ray fluorescence spectrometer.

The attention of astronomers has been focusing upon Cyg X-1. Cyg X-1 has been identified with a massive BO star (ref. 19-22), the spectrum of which indicates a binary star system. The identification has strengthened the case of those who argue that a "black hole" is involved in the X-ray production. According to their models, X-rays originate from the accretion of matter upon a dark binary companion of the massive star. From the period of the binary system as determined by periodic Doppler shifts in the visible line spectrum, the mass of the dark companion of the BO star can be inferred to be significantly greater than one solar mass. The fast time variability in the X-ray luminosity of Cyg X-1 (significant changes in less than 1 sec (ref. 19-25)) requires that the dark companion be compact; that is, have a radius no larger than that of a white dwarf. According to present theories of stellar structure, a star as massive as the binary companion of the BO star cannot exist in a stable form as a white dwarf or even as a neutron star. A black hole appears to be the only acceptable alternative. For this reason, Cyg X-1 is perhaps the most provocative of all galactic X-ray sources; consequently, about half the available Apollo 16 pointing time was devoted to it.

The remainder of the pointing time was devoted to observing Sco X-1, the most intense of all observed galactic X-ray sources. A single Apollo 15 observation of Sco X-1 of 26-min duration indicated the presence of a variability on a time scale of several minutes that suggested further investigation. More favorable thermal conditions for Sco X-1 at the time of the Apollo 16 mission plus a better understanding from the Apollo 15 experience of the thermal behavior of the spacecraft during extended periods of pointing permitted longer observations of approximately 2 hr.

By observing Sco X-1 and Cyg X-1 for the first time continuously for 2 hr in coordination with ground-based optical and radio astronomers, it was hoped that more could be learned about the X-ray emission processes. Specifically, it was hoped to determine that Cyg X-1 and Sco X-1 are similar-appearing objects on time scales of more than several seconds and that they are examples of related objects under somewhat different physical conditions. For example, in the case of Sco X-1, a thin atmosphere could disperse the subsecond time variability seen in Cyg X-1 but not affect slower time changes.

Results

Sco X-1.—Some results are available from preliminary analysis of the Apollo 16 data. Figures 19-6(a) and 19-6(b) show the temporal behavior of Sco X-1 during the first two observation periods, respectively. Significant changes in count rate originate partly from Sco X-1 and partly from motion of the spacecraft. The motion of the spacecraft, as indicated by the angle of the detector axis with respect to the

celestial location, is shown for comparison in figure 19-6. Although spacecraft steadiness was well within the nominal Apollo capability, spacecraft motion does appear to be reflected in the variation of count rate. However, there are important changes in the count rate of Sco X-1 that cannot be explained by spacecraft motion.

The first sighting of Sco X-1 was made from 03:34 to 04:04 G.m.t. on April 25. During this time, the spacecraft motion showed little uniformity. Variations in the polar angle occurred with amplitudes of $\pm 0.1^\circ$ to $\pm 0.5^\circ$ and periods of 1 to 5 min. The mean polar angle during the sighting was approximately 7° as was planned. The large increase in the counting rate from 03:39 to 03:49 G.m.t. occurred during a time of minimum spacecraft motion.

The second sighting of Sco X-1 was made from 02:14 to 04:52 G.m.t. on April 26. During the course of this sighting, four distinct and separate types of spacecraft motion were discernible. From 02:14 to 02:52 G.m.t., the motion was characterized by regular variations of large amplitudes of $\pm 0.5^\circ$ and periods of 2 min, with a mean polar angle of approximately 6.6° between Sco X-1 and the normal to the detector face. From 02:52 to 03:39 G.m.t., the variations were irregular with amplitudes of 0.1° to 0.8° and separations of 1 to 7 min between peaks. The mean polar angle remained at approximately 6.6°. At 03:39 G.m.t., the mean angle shifted to 6.9° and the amplitude of the variations decreased to 0.1° to 0.3° with a peak separation of 1 to 5 min. The motion again became regular and periodic at 04:06 G.m.t., with an amplitude of $\pm 0.2^\circ$, a period of approximately 1 min, and a mean polar angle of 6.9°. This motion continued until the end of the second sighting.

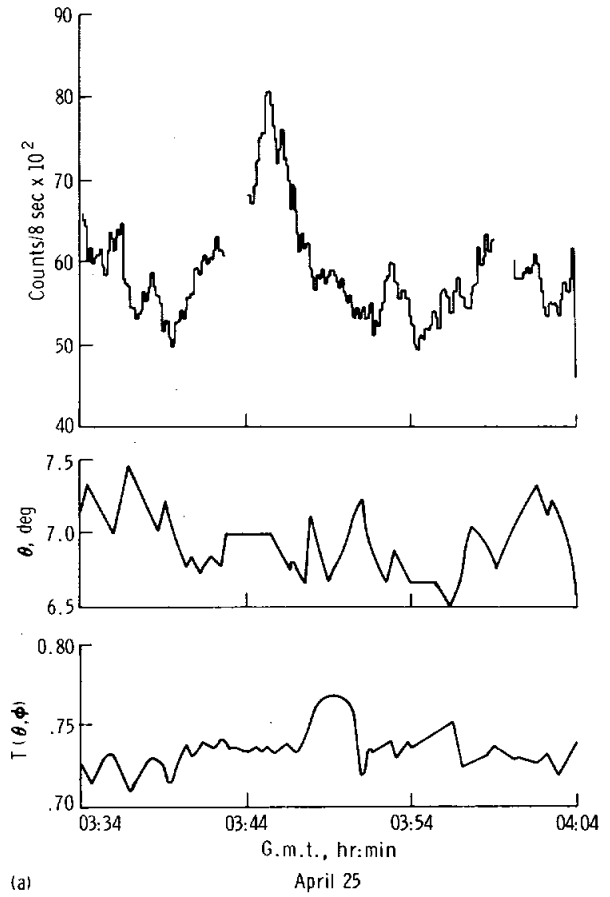

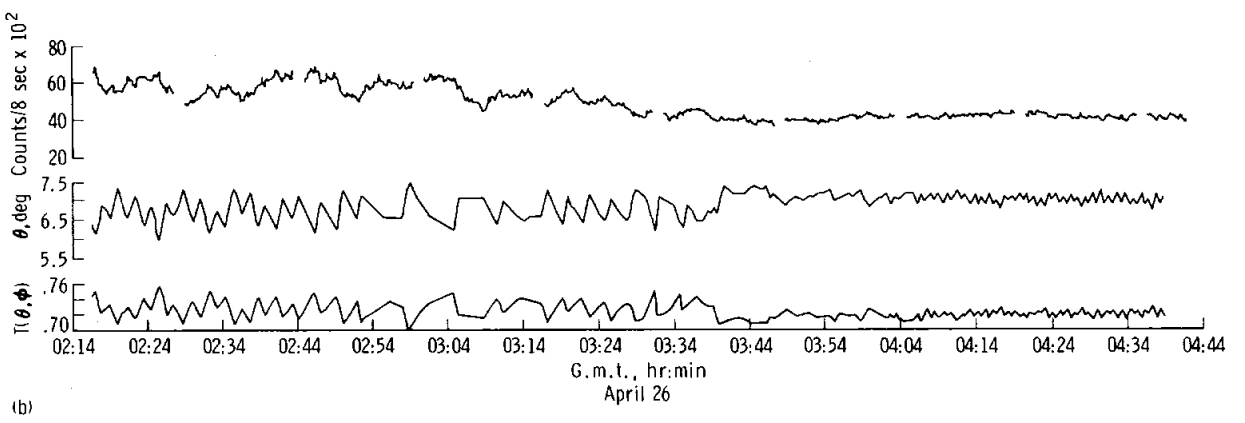

FIGURE 19-6.–Variations of count rate from Sco X-1. The spacecraft motion as reflected by changes in the polar angle θ is shown as well as its expected effect upon the counting efficiency $T(\theta, \phi)$. (a) First observation. (b) Second observation.

In general, Sco X-1 was active during the first sighting. After allowing for spacecraft motion, significant changes (10 to 30 percent) in its intensity could be identified in a few minutes. Because of a late change in the scheduled time for the first sighting of Sco X-1, there was no simultaneous optical or radio data. However, reports received from the McDonald and Algonquin Observatories indicate that Sco X-1 was active optically and in radio for at least several hours following the Apollo 16 observation. Flare activity was detected at the ground observatories. There was continued activity at the beginning of the second observation of Sco X-1; during the final hour, the count rate settled down and was relatively constant.

Cyg X-1.–Two observations of Cyg X-1 were made during the Apollo 16 mission. Figure 19-7 shows the variation of count rate during the second observation. There are two large increases in count rate. However, neither of these appears to be intrinsic to Cyg X-1. The pulse shape discriminator (PSD) channel shown in the lower portion of figure 19-7 is conditioned primarily by the strength of the particle background. It is also affected by X-rays with $E > 7$ keV. The fact that the PSD channel exhibits a stronger counting rate change than the two energy ranges is probably an indication of a sudden increase in the particle background. The spacecraft encountered two pulses of electrons or protons (or both) of durations of approximately 2 to 5 min in cislunar space. It may be possible that hard X-ray flares have occurred in Cyg X-1, but the particle interpretation is more likely.

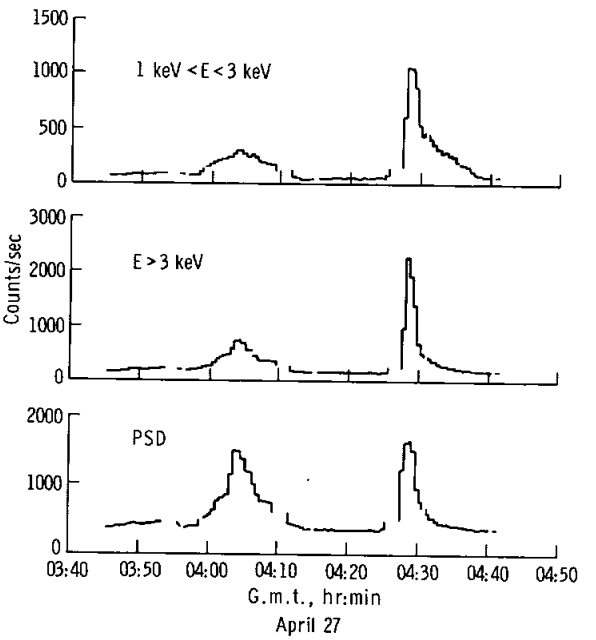

FIGURE 19-7.–Count rate during the second Apollo 16 observation of Cyg X-1. The two large increases in rate at 04:05 and 04:28 G.m.t. are probably particle effects in cislunar space because the PSD rates also increase.

In addition to the effect described previously, there is a significant change in the mean intensity of Cyg X-1 between two Apollo 16 observations. Table 19-IV summarizes this difference. The near equality between the PSD count rates of the two observations (prior to the particle events) indicates that the particle background is the same. Cyg X-1 is twice as

TABLE 19-IV.–Count Rates During Cygnus X-1 Observations

Energy channel	*Apollo 15 (a)*	*Apollo 16*	
		First observation	*Second observation (b)*
3 keV $> E >$ 1 keV	260	360	750 → 2 500 ↘ 8 600
$E >$ 3 keV	900	860	1500 → 5 800 ↘ 18 000
PSD	3000	2900	3100 → 12 000 ↘ 13 000

[a]Units are counts/8 sec.

[b]The first set of values is the average count rate; the second and third numbers refer to each of two particle event intensities.

intense in the second observation. The slight excess of PSD events, 3100 as compared to 2900, can be explained as a doubling of the number of events in the range above 7 keV.

Conclusions

The following conclusions can be made from the pointed observations of Sco X-1 and Cyg X-1.

(1) Sco X-1 is characterized by quiet periods and by periods in which there are intensity changes of approximately 10 to 30 percent in a few minutes. The active periods can last for at least a day.

(2) When Sco X-1 shows changes in X-ray intensity, there are concurrent but not necessarily simultaneous changes in its optical and radio intensity.

(3) Cyg X-1 can double in intensity within a day or so, an increase which is larger than the observed changes in Sco X-1. The increase occurs in all three energy ranges: 1 to 3 keV, >3 keV, and >7 keV. The average intensity of Cyg X-1 over a several-minute interval can remain relatively stable for at least an hour.

(4) The time variability of Sco X-1 and Cyg X-1 does not appear to be similar in the time regime of several seconds to 2 hr. Although Cyg X-1 exhibits subsecond pulsations during its active periods, Sco X-1 has greater variability on a time scale of a few minutes than Cyg X-1 as it appears during the Apollo 16 mission.

(5) Transient particle effects that last several minutes exist in cislunar space. The strength of the two events observed during the Apollo 16 mission is approximately 100 particles/cm^2-sec. These events can lead to background problems in instruments with broad fields of view and can simulate flares in X-ray stars.

REFERENCES

19-1. Adler, I.; Trombka, J.; Gerard, J.; Lowman, P.; et al.: Apollo 15 Geochemical X-Ray Fluorescence Experiment: Preliminary Report. Science, vol. 175, no. 4020, Jan. 28, 1972, pp. 436-440.

19-2. Adler, I.; Trombka, J.; Gerard, J.; Schmadebeck, R.; et al.: X-Ray Fluorescence Experiment. Sec. 17 of Apollo 15 Preliminary Science Report. NASA SP-289, 1972.

19-3. Adler, I.; Gerard, J.; Trombka, J.; Schmadebeck, R.; et al.: The Apollo 15 X-Ray Fluorescence Experiment. Proceedings of the Third Lunar Science Conference, vol. 3, David R. Criswell, ed., MIT Press (Cambridge, Mass.), 1972.

19-4. Levinson, A. A., ed.: Proceedings of the Second Lunar Science Conference. MIT Press (Cambridge, Mass.), 1971.

19-5. Apollo 15 Preliminary Examination Team: The Apollo 15 Lunar Samples: A Preliminary Description. Science, vol. 175, no. 4020, Jan. 28, 1972, pp. 363-375.

19-6. Levinson, A. A., ed.: Proceedings of the Apollo 11 Lunar Science Conference. Pergamon Press (New York), 1970.

19-7. McKay, D. S.; Morrison, D. A.; Clanton, U. S.; Ladle, G. H.; and Lindsay, J. F.: Apollo 12 Soil and Breccia. Proceedings of the Second Lunar Science Conference, vol. 1, A. A. Levinson, ed., MIT Press (Cambridge, Mass.), 1971, pp. 755-774.

19-8. Meyer, C.; Brett, R.; Hubbard, N. J.; Morrison, D. A.; et al.: Mineralogy, Chemistry, and Origin of the KREEP Component in Soil Samples From the Ocean of Storms. Proceedings of the Second Lunar Science Conference, vol. 1, A. A. Levinson, ed., MIT Press (Cambridge, Mass.), 1971, pp. 393-412.

19-9. Turkevich, Anthony L.; Patterson, James H.; and Franzgrote, Ernest J.: Chemical Analysis of the Moon at the Surveyor VI Landing Site: Preliminary Results. Science, vol. 160, no. 3832, Jan. 7, 1968, pp. 1108-1110.

19-10. Mason, Brian; and Melson, William G.: The Lunar Rocks. John Wiley & Sons, Inc., 1970, p. 11.

19-11. Turkevich, Anthony L.; Franzgrote, Ernest J.; and Patterson, James H.: Chemical Analysis of the Moon at the Surveyor V Landing Site: Preliminary Results. Science, vol. 158, no. 3801, Nov. 3, 1967, pp. 635-637.

19-12. Vinogradov, A. P.: Preliminary Data on Lunar Ground Brought to Earth by Automatic Probe Luna-16. Proceedings of the Second Lunar Science Conference, A. A. Levinson, ed., MIT Press (Cambridge, Mass.), 1971, pp. 1-16.

19-13. Lunar Sample Preliminary Examination Team: Preliminary Examination of Lunar Samples From Apollo 14. Science, vol. 173, no. 3998, Aug. 20, 1971, pp. 681-693.

19-14. Wood, J. A.; Marvin, U. B.; Powell, B. N.; and Dickey, J. S., Jr.: Mineralogy and Petrology of Apollo 11 Samples. Smithsonian Astrophysical Observatory Special Rept. 307, Jan. 1970. (Also available as NASA CR-107932, Jan. 1970.)

19-15. Marvin, U. B.; Wood, J. A.; Taylor, G. J.; Reid, J. B.; et al.: Relative Proportions and Probable Sources of Rock Fragments in the Apollo 12 Soil Samples. Proceedings of the Second Lunar Science Conference, vol. 1, A. A. Levinson, ed., MIT Press (Cambridge, Mass.), 1971, pp. 679-700.

19-16. Turkevich, Anthony L.; Franzgrote, Ernest J.; and Patterson, James H.: Chemical Analysis of the Moon at the Surveyor VII Landing Site: Preliminary Results. Science, vol. 162, no. 3849, Oct. 4, 1968, pp. 117-118.

19-17. Whitaker, E. A.: The Surface of the Moon. Sec. 3 of The Nature of the Lunar Surface; Proceedings of the 1965 IAU-NASA Symposium, Wilmot N. Hess, Donald H. Menzel, and John A. O'Keefe, eds., Johns Hopkins Press (Baltimore), 1966, pp. 79-98.

19-18. Gault, D. E.; Adams, J. B.; Collins, R. J.; Kuiper, G. P.; et al.: Lunar Theory and Processes. Sec. 9 of Surveyor

VII, A Preliminary Report. NASA SP-173, May 1968.

19-19. Pohn, H. A.; and Wildey, R. L.: A Photoelectric-Photographic Study of the Normal Albedo of the Moon, Accompanied by an Albedo Map of the Moon by H. A. Pohn, R. L. Wildey, and G. E. Sutton.(Contributions to Astrogeology). U.S. Geological Survey Professional Paper 599-E, 1970.

19-20. Milton, Daniel J.; and Hodges, Carroll Ann: Geologic Map of the Descartes Region of the Moon. Geol. Atlas of the Moon, Apollo 16 Pre-Mission Map, Sheet 1. U.S. Geol. Survey Misc. Geol. Inv. Map I-748, 1972.

19-21. Head, James W., III; and Goetz, Alexander F. H.: Descartes Region: Evidence for Copernican-Age Volcanism. J. Geophys. Res., vol. 77, no. 8, Mar. 10, 1972, pp. 1368-1374.

19-22. Webster, B. Louise; and Murdin, Paul: Cygnus X-1 – A Spectroscopic Binary With a Heavy Companion? Nature, vol. 235, no. 5332, Jan. 7, 1972, pp. 37-38.

19-23. Bolton, C. T.: Identification of Cygnus X-1 with HDE 226868. Nature, vol. 235, no. 5336, Feb. 4, 1972, pp. 271-273.

19-24. Schreier, E.; Levinson, R.; Gursky, H.; Kellogg, E.; et al.: Evidence for the Binary Nature of Centaurus X-3 From UHURU X-Ray Observations. Astrophys. J. (Letters), vol. 172, no. 3, pt. 2, Mar. 15, 1972, pp. L79-L89.

19-25. Oda, M.; Gorenstein, P.; Gursky, H.; Kellogg, E.; et al.: X-Ray Pulsations From Cygnus X-1 Observed From UHURU. Astrophys. J. (Letters), vol. 166, no. 1, pt. 2, May 15, 1971, pp. L1-L7.